

# Self-organized localization of macrostates by additive noise in a fast-slow dynamical system: Effect of the slow nonreactive mode on the barrier crossing rate of the fast, bistable mode

Vladimir Chinarov and Michael Menzinger

*Department of Chemistry, University of Toronto, Toronto ON, Canada M5S 3H6*

(Received 9 December 1999)

We have studied the stochastic dynamics of a two-dimensional gradient system composed of a fast, bistable mode and a slow, monotonically decaying mode. The coupling is bidirectional and cooperative. Additive white noise acts on the fast mode only. We find that the noise intensity controls the location of macrostates (shape of the probability density function), the appearance of bimodality in the slow-mode probability distribution and, together with the coupling strength, the rate of fast-mode barrier crossing. These features arise from the interplay of noise, widely separated time scales, and bidirectional, excitatory coupling. They are believed to be generic.

PACS number(s): 05.40.-a

## I. INTRODUCTION

The stochastic dynamics of two-dimensional (2D) systems with widely separated time scales has provided insights [1–5] into the ways in which external noise may qualitatively and quantitatively alter and control their deterministic dynamics. Minimal dynamical models may be obtained through (adiabatic) elimination of fast modes that are nonessential to the qualitative dynamics. In this sense, the model composed of a fast, bistable and a slow, monostable mode, which we study in this paper, lies at the limit of adiabatic reducibility. Embedded in a fluctuating environment, such a system may be viewed as representing the fast reactive and slow nonreactive modes of a large biomolecule [5]. It is also related to a model of the gating dynamics of ion channels in biomembranes [6,7].

Since “interesting” stochastic effects, such as shifts of probability density functions and their peaks, the macroscopic states [8], the appearance of noise-induced bistability [9] and stabilization of unstable states [10,11], require the action of multiplicative noise as long as the system is one-dimensional, many of the studies of stochastic dynamics of 2D systems were performed with multiplicative noise. But in higher dimensional dynamical systems, bidirectional mode-coupling (Fig. 1) may lead to a qualitatively similar, effectively quasimultiplicative response, even if the noise is additive.

A further issue is the influence of slow, nonreactive mode(s) on the barrier-crossing dynamics of the fast reactive mode, a Brownian particle moving in a double-well potential [12]. The problem of relaxation of a probability distribution, located initially at the maximum of a double-well potential, as well as the problem of diffusion in stochastic systems were studied by many authors in one-dimensional [13–15] and multidimensional cases [16–18].

The goal of this paper is to study the dynamics of a system composed of a fast, bistable mode that is linearly, symmetrically and cooperatively coupled to a slow, nonreactive mode under the influence of additive noise acting on the fast subsystem. For convenience, this system may be formulated

as a gradient system based on a potential  $V(q, Q)$ . It is formally related to the Fitzhugh-Nagumo (FN) model of neuronal firing [19,20] except that the variables in the latter are asymmetrically and antagonistically coupled. This prevents the FN model from being a gradient system.

We find that the system’s nontrivial stochastic dynamics is governed by the interplay of the asymmetry of noise applied to fast system only (thermal gradient), the time-scale separation and the nature of the coupling. This dynamics manifests itself as follows: (1) Through the noise-induced shift of the probability density function (PDF) whose maxima correspond to the most probable macroscopic states [11]. In other words, the noise-induced macrostates may be localized in phase space [8,10,11], where noise acts as the control parameter. (2) In a certain range of parameter space that includes the noise intensity, the slow-mode probability distribution is unimodal at low and at high values of noise, but at intermediate levels of noise it develops a second maximum—the phenomenon of noise-induced bistability [9,11]. (3) Closely related to these transformations of the stationary probability density is the modification of transition rates in the bistable, fast mode and of the relaxation time from the top of the saddle point of the potential to the stochastic macrostate by the nonreactive mode. We find evidence of noise-induced “locking” of the system in the reactant well due to the localization of the slow mode, of noise-induced stabilization [8] of the unstable state at the top of the barrier, and of noise-induced slowing-down [21,22] of the relaxation rate.

The paper is organized as follows. In Sec. II, we introduce the dynamical model, and analyze it numerically in Sec. III. In particular, we study the relevant probability density distributions, i.e., their change in position and topology as a func-

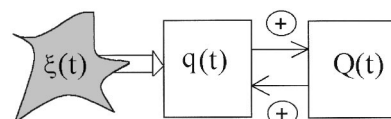


FIG. 1. Schematic of the energy flow from the heat bath into the fast subsystem followed by bidirectional coupling and dissipation.

tion of noise intensity, and their relaxation to an asymptotic, stationary distribution. The numerical results are then compared with approximate solutions of the relevant Fokker-Planck equation derived in Appendix A. The second focus is the study of the rate of the fast mode barrier crossing in the presence of the slow mode. The barrier-crossing rate is compared with the 1D Kramers' result. Finally, we study the relaxation from the saddle point to the stationary macrostate. The results are summarized and discussed in Sec. IV.

## II. MODEL AND BASIC EQUATIONS

Consider the following dynamical system composed of a fast, bistable mode  $q$  and a slow, linearly decaying mode  $Q$ . They are linearly coupled, subjected to noise, and dimensionless:

$$\partial q / \partial t = q - q^3 + c_1 Q + \sqrt{2D_1} \xi_1(t), \quad (1a)$$

$$\tau^{-1} \partial Q / \partial t = -Q + c_2 q + \sqrt{2D_2} \xi_2(t), \quad (1b)$$

where  $c_1, c_2$  are the coupling strengths and  $\tau (\tau \ll 1)$  is the time-scale parameter.  $D_1, D_2$  are the intensities of the statistically independent, additive stochastic forces  $\xi_1(t), \xi_2(t)$ , where  $\xi(t)$  is a Gaussian white noise defined by  $\langle \xi_i(t) \rangle = 0$ ,  $\langle \xi_i(t) \xi_j(t') \rangle = \delta_{ij} \delta(t - t')$ . In the general case, the subsystems have different temperatures [12]. Here we study the nontrivial dynamics of the limiting case  $D_2 = 0$ . The opposite case  $D_1 \ll D_2$  was studied in a Hamiltonian system [12,23]. The bistable mode  $q$  represents a reaction coordinate—one well (say, the left one) corresponding to reactants and the other one to products. The slow, monotonically decaying variable  $Q$  may be considered as a nonreactive mode.

The signs of the coupling coefficients  $c_1, c_2$  determine different classes of dynamical model. When the coupling coefficients have opposite signs, the interactions may be either excitatory ( $c_1 > 0$ ), or inhibitory ( $c_1 < 0$ ). Such systems cannot be gradient systems. A well-known example is the Fitzhugh-Nagumo model [19,20], defined by Eq. (1),  $c_1 > 0$  and  $c_2 < 0$ . Stochastic versions of the FN model with  $D_2 \ll D_1$  have been studied [4,5,24].

By a change of variables, Eq. (1) may be transformed into a gradient system as outlined in Appendix B [Eq. (B2)] when both coupling coefficients are positive ( $c_1, c_2 > 0$ ), i.e., with cooperative (excitatory) type of interactions. The corresponding potential  $V(q', Q'; c, \tau)$  is shown in Fig. 2. The numerical studies were, however, done using the original, untransformed coordinates and Eq. (1) using an excitatory type of coupling:  $c_1 = c_2 = c > 0$ .

## III. NUMERICAL STUDIES

Different realizations of the processes  $q(t)$  and  $Q(t)$  were obtained by solving Eq. (1) by a fourth-order stochastic Runge-Kutta algorithm [25]. The integration time step was  $h = 0.01$ . The cumulative PDF  $P(q, Q) \Delta V$  characterizes the statistical properties of the system by following a single trajectory over a long time, and counting the frequency with which it visits a volume element  $\Delta V$  of phase space. The bin width was taken as 0.08 for  $q$  and 0.024 for  $Q$ .

Keeping in mind that all simulations were made for the nongradient case described by Eq. (1) to analyze some sym-

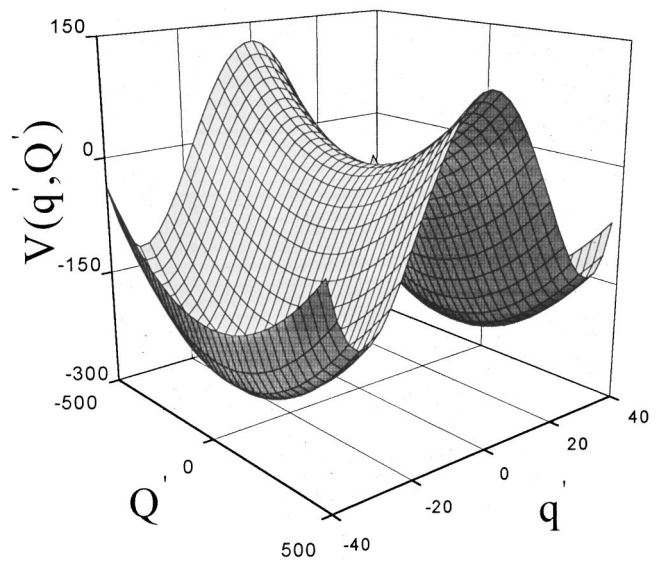


FIG. 2. The potential  $V(q', Q'; c, \tau)$  at  $c = 0.5$ ,  $\tau = 0.001$ , scaled  $q', Q'$  (Appendix B). Dimensionless units are used hereafter.

metry properties of the probability density function, we consider briefly the gradient system described by Eq. (B2). In the noise-free case  $D = 0$ , the system settles into the potential minima at  $(q'_{\min}, Q'_{\min})$ , which are symmetric with respect to the origin but asymmetric at constant slow coordinate  $Q' = \text{const}$ . Consequently, the probability density  $P(Q', q'; c, \tau, D)$  at nonzero noise is also asymmetric for a wide range of  $c, \tau$  and  $0 < D < D_1$  and becomes symmetric only above some value  $D_1$  of noise. Figure 3 illustrates this asymmetry of the stationary (asymptotic) probabilities  $P^s(q), P^s(Q)$  for  $D = 0.16$  (unscaled variables  $Q, q$  are used hereafter). Since the mean value of the slow mode  $\langle Q \rangle \neq 0$  [and the potential  $V(q', \langle Q \rangle)$ ] is asymmetric at this noise level, the fast subsystem spends more time in the left well of the potential (Fig. 2). This asymmetry depends on the sign of the coupling constants—reversing their sign also inverts the population of the wells [Fig. 3(c)].

Figure 4 traces the evolution of this bimodality in  $Q$  through the nonstationary PDF  $P(q, Q; N)$  for different values of the observation time given by  $t = Nh$ , where  $N$  is the number of integration time steps. The initial conditions for slow and fast variables [Fig. 4(a)] were taken at their negative steady-state values [see Eq. (1)] in the absence of noise,  $q(0) = -\sqrt{1 + c^2}$ ,  $Q(0) = q(0)c$ . The three panels show  $P(q, Q; N)$  for  $N = 1.0E8, 3.0E8, 5.0E9$ , and the asymptotic approach to the stationary distribution that we denote as  $P^s(q, Q)$ . A further increase beyond  $N = 5.0E9$  does not change the probability of panel (c). We should underline that the asymptotic stationary distribution  $P^s(q, Q)$  is asymmetric [Fig. 4(c)], with its highest peak located in the left well of  $V(q) = -q^2/2 + q^4/4$ . The same asymmetric distribution will be reached regardless of initial conditions. Therefore, there exists no  $P^s(q, Q)$  that is symmetric to that shown in Fig. 4(c). Such symmetry could however, be achieved [as shown in Fig. 3(c)] by inverting the signs of both coupling coefficients in Eq. (1), changing the nature of coupling from excitatory ( $c_i > 0$ ) to inhibitory ( $c_i < 0$ ).

A possible reason of the observed asymmetry may be connected with an interplay of three factors—random forc-

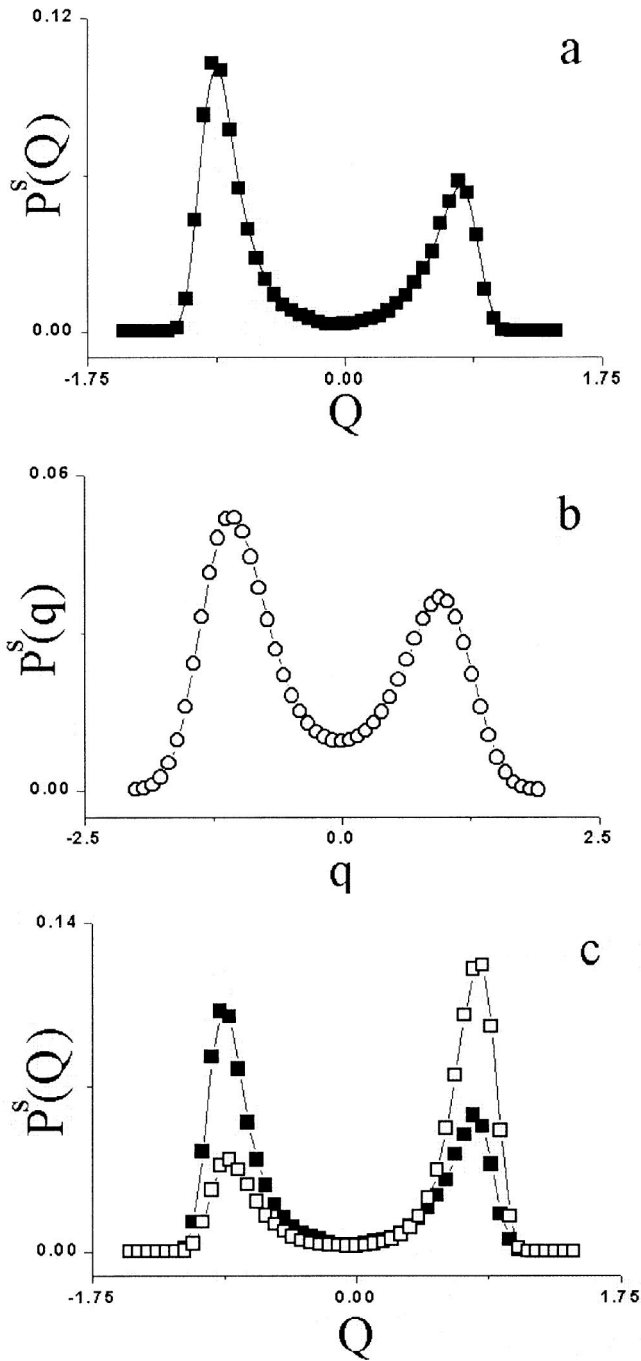


FIG. 3. Stationary probability density functions  $P^s(Q), P^s(q)$  for parameters:  $D=0.16, c=0.5, \tau=0.001$ . (a): slow-mode probability  $P^s(Q)$ ; (b): fast-mode probability  $P^s(q)$ ; (c): fast-mode probability is inverted upon changing from symmetric, cooperative coupling ( $c=0.5$ ; full squares) to symmetric inhibitory coupling ( $c=-0.5$ ; empty squares).

ing, the type of interaction between slow and fast subsystems, and different time scales for them. For high noise ( $D > 0.18$ ), the fast mode switches between its stable states in a way typical for noisy driven bistable systems [2,15] (see below). For the noise intensity  $D \sim 0.18$ , depending on the phase relation of the random force, slow and fast modes, the slow subsystem tends to negative (for  $c > 0$ ) or positive (for  $c < 0$ ) steady states (and fluctuates around them), while the fast subsystem spends most of its time in the left or right

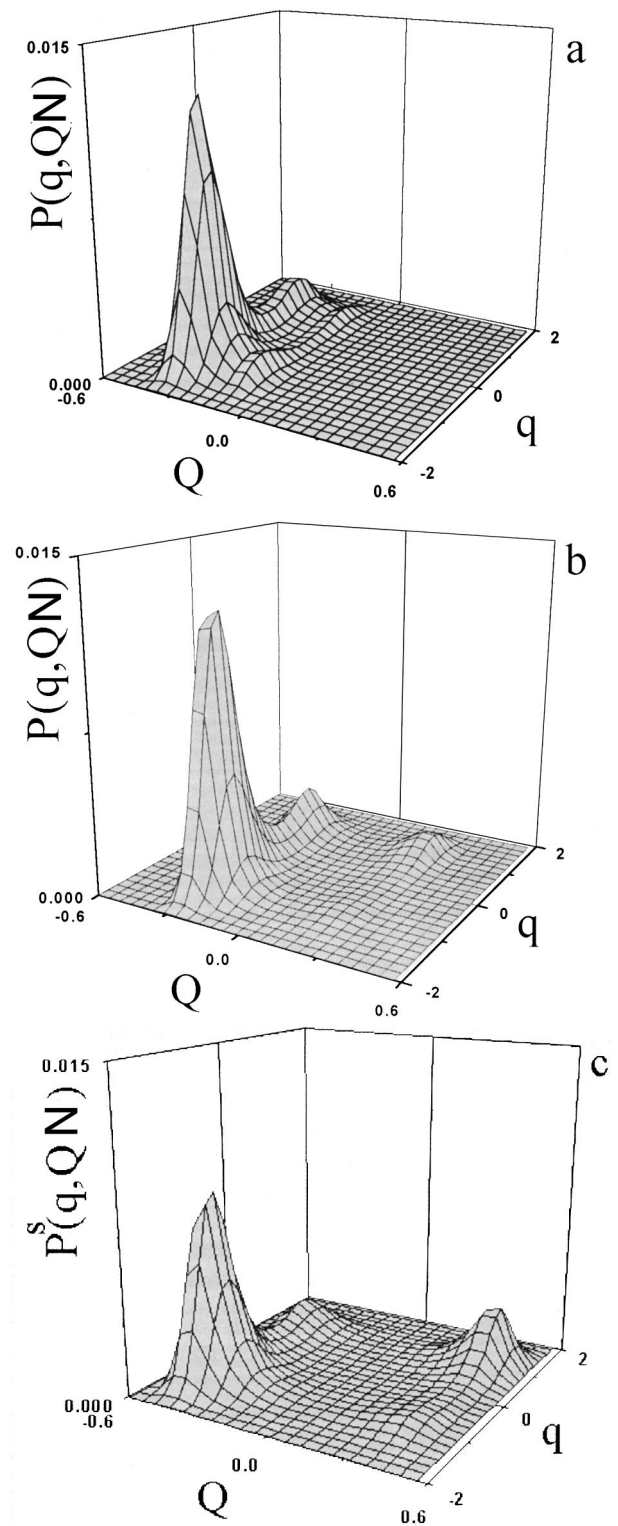


FIG. 4. Time evolution of the cumulative PDF  $P(q, Q, N)$  for  $D=0.18, c=0.5, \tau=0.001$ . (a)  $N=1.0 \times 10^8$ ; (b)  $N=3.0 \times 10^8$ ; (c)  $N=5.0 \times 10^9$ . For (c) the PDF is stationary.

well of the double-well potential  $V(q)$ .

A detailed study of the parameter dependencies of the asymptotic PDF  $P^s(q, Q; D, c, \tau)$  reveals further interesting features. Noise-induced bistability appears in the slow mode  $Q$  over a narrow range  $D_1 < D < D_2$  of noise, centered near  $D \approx 0.18$ . Three relevant cases are shown in Fig. 5: (a) subcritical  $D < D_1$ , (b) bistable  $D_1 < D < D_2$ , and (c) supercritical

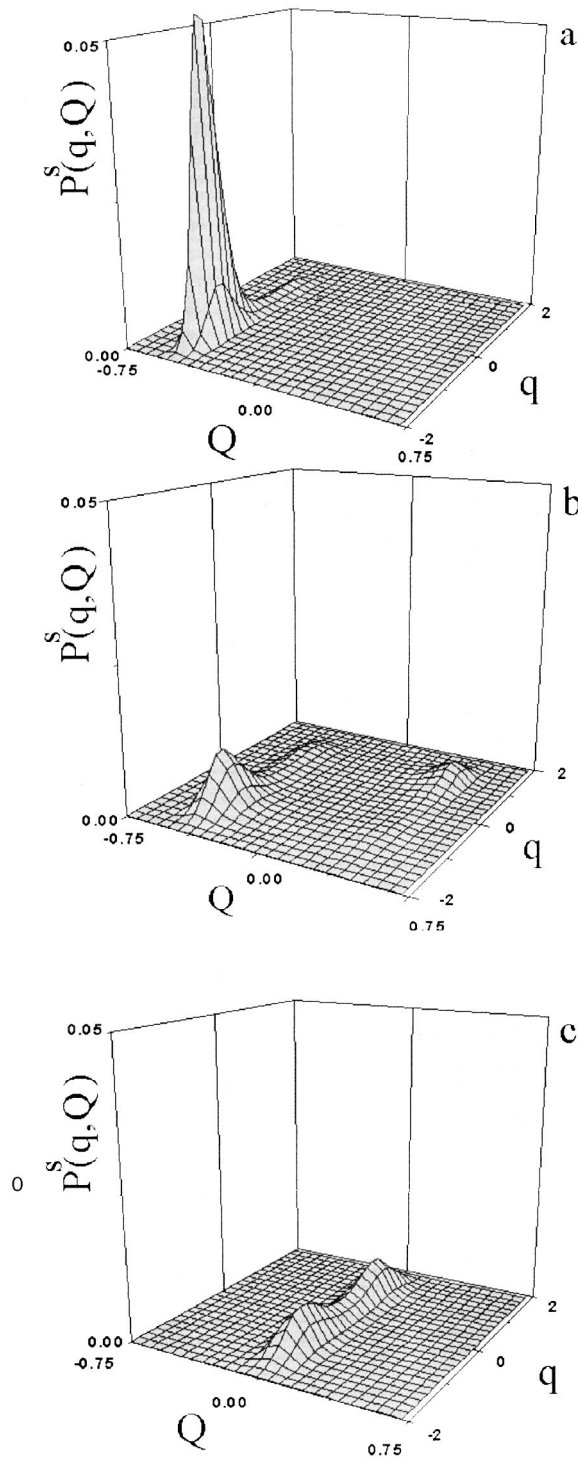


FIG. 5. Dependence of the stationary PDF $P^s(q, Q)$  on noise intensity at  $\tau=0.001$ ,  $c=0.5$ . (a):  $D=0.13$ ; (b):  $D=0.18$  (noise-induced bistability); (c):  $D=0.28$ .

cal  $D > D_2$ . Panel (a) ( $D=0.13$ ) shows pronounced asymmetry of the fast mode and a unimodal distribution of the slow mode. Panel (b) ( $D=0.18$ ) illustrates the bimodal distributions and asymmetries of both fast and slow probability densities. In panel (c) ( $D=0.28$ ) the slow mode is again unimodal, this time centered near  $\langle Q \rangle = 0$ , and the fast mode is now symmetrically bimodal. At higher values of noise, the distribution  $P(Q)$  becomes Gaussian.

To illustrate how the macrostate can be guided along the

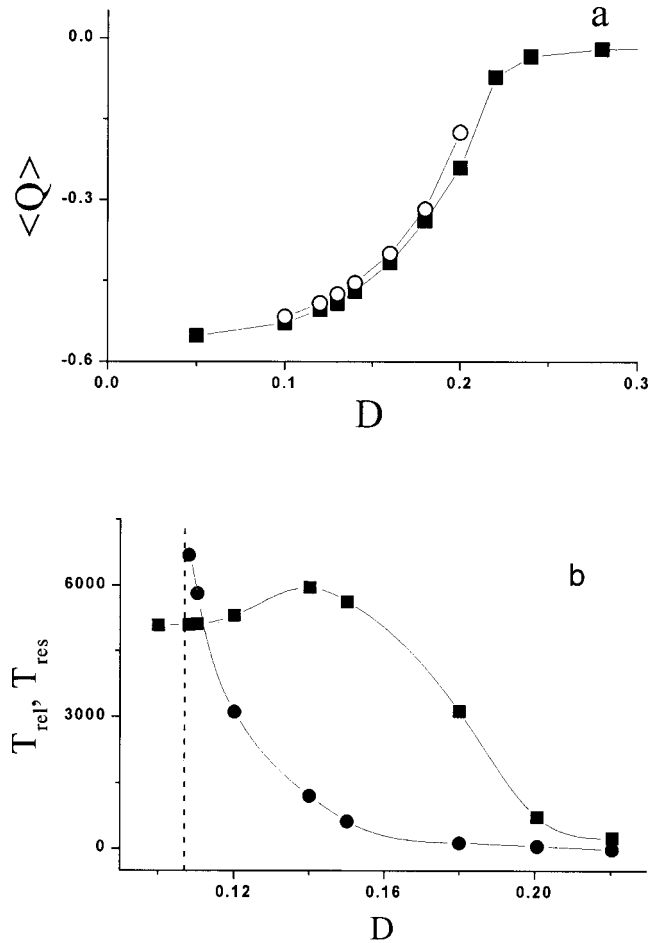


FIG. 6. (a) Dependence of the location  $\langle Q \rangle$  of the slow-mode stationary PDF maximum on noise  $D$  for  $c=0.5$ ,  $\tau=0.001$ . Full squares: numerical results. Open circles: analytical prediction from Fokker-Planck equation (A1, A4). (b) Dependence of mean relaxation time  $\langle T_{rel} \rangle$  (full squares) and mean residence time  $\langle T_{res} \rangle$  (full circles) on noise  $D$ . Parameters as in (a).

slow coordinate under the control of noise, Fig. 6(a) shows the position of the most probable value  $\langle Q \rangle$  of the slow variable as a function of noise  $D$ . In terms of the gradient case description [with a potential function given by Eq. (B1)], this means that noise “pumps” the system from  $Q'_{min} = (1 + c^2)^{1/2}c/\tau$ , the minimum of the potential, toward  $\langle Q \rangle \approx 0$  in the limit of high noise. The shift of the macrostate from the potential minimum to  $\langle Q \rangle \approx 0$  has the appearance of a phase transition, with a turning point near  $D \approx 0.18$ . At this point, the susceptibility to noise is maximal and noise-induced bistability occurs in its neighborhood. The noise-induced macrostates  $\langle Q \rangle$  (solid squares) agree well with the theoretical steady-state solutions (open circles) of the corresponding Fokker-Planck equation (A1). The latter were obtained using the approximations described by Eqs. (A2) and (A3). The noise dependence of the asymptotic PDF reflects the stationary aspect of the problem.

A related locking of the fast-mode kinetics by the slow mode manifests itself in the reverse process—the relaxation from the saddle point of the potential to the stochastic steady state. The mean relaxation time  $\langle T_{rel} \rangle$  is obtained as the average over many realizations of the time required to reach the previously calculated stochastic macrostate  $\langle Q(D) \rangle$ , starting

from the saddle point. Figure 6(b) (full squares) shows the corresponding mean relaxation time  $\langle T_{\text{rel}} \rangle$  as a function of noise intensity. The curve is strongly nonmonotonic and has the following features: At low noise,  $\langle T_{\text{rel}} \rangle$  is rather high and constant, and with increasing  $D$ ,  $\langle T_{\text{rel}} \rangle$  increases further and goes through a maximum near  $D \approx 0.15$ , after which it decreases sharply (halfway point at  $D \approx 0.18$ ) to a value near zero. The lengthening of the relaxation time above the low-noise value reflects the phenomenon of noise-induced slowing-down, which was described and analyzed elsewhere [21,22]. The subsequent, sudden shortening of the relaxation time at  $D > 0.15$  is related to the gradual shift of the target macrostate  $\langle Q(D) \rangle$  toward the barrier, i.e., to the shortening of the relaxation path.

Figure 6(b) (full circles) shows the dependence of the mean residence time  $\langle T_{\text{res}} \rangle$  on noise intensity  $D$ . This is the average time the system spends in the reactant well before escaping from it by crossing the barrier. With decreasing  $D$  it rises exponentially [Fig. 7(a)] and asymptotically approaches infinity at some value of  $D > 0.1$  (shown schematically by a dashed line). This reflects the fact that the diffusion process is highly localized and the slow variable  $Q$  never crosses the saddle point, while the fast variable  $q$  spends much more time in one of the wells.

Closely related to the shape of the probability density function is the role of the slow, nonreactive mode on the rate of barrier crossing and of relaxation from the barrier top. For this kinetic aspect we calculated the mean residence times  $\langle T_{\text{res}} \rangle$  in the reactant well from single, long trajectories of the 2D system (2,3) and compared them with theoretical predictions [26] for the symmetric, 1D double-well problem.

Figure 7(a) shows the dependence of  $\langle T_{\text{res}} \rangle$  on noise intensity in Arrhenius representation, for four values of the coupling constant  $c$ . The Arrhenius parameters are defined by  $\langle T_{\text{res}} \rangle = T_{\infty} \exp(\Delta E/D)$ . The result for the uncoupled ( $c = 0$ ) case, marked by open circles agrees almost perfectly with the theoretical Kramers' prediction  $T_{\text{res}} = (\pi/\sqrt{2}) \exp(0.25D)$  for the 1D white noise case [26] depicted by the line. As the coupling strength increases from  $c = 0$  to  $c = 0.1, 0.3, 0.5$ , the slope or apparent activation energy  $\Delta E$  increases nonlinearly, while the preexponential factor  $T_{\infty}$  decreases almost linearly, as shown in Fig. 7(b). Both cooperate in the slowing-down or locking of the fast mode barrier-crossing rate by its coupling to the slow mode. This locking of the barrier-crossing rate is particularly pronounced for  $c = 0.3, 0.5$ , where the apparent activation energy increases more rapidly than linearly. This relates to the fact that the probability density  $P(q, Q)$  is highly asymmetric and unimodal under these conditions [see Fig. 5(a)].

The slow relaxation at  $D < 0.15$  [Fig. 6(b)] is the kinetic aspect of the steady-state observation [Fig. 5(a)] that the over-the-barrier process does not penetrate into the product region. For  $D > 0.15$ , however, the slow-mode distribution begins to show bimodality and the flux penetrates into the product region. At the turning point  $D = 0.18$  of Fig. 7(b), bimodality of  $P_s(Q)$  is fully developed [Fig. 5(b)], but  $\langle Q \rangle$  has not yet reached the saddle point and  $P(Q)$  remains asymmetric.

#### IV. SUMMARY AND DISCUSSION

We have studied the stochastic dynamics of a system composed of a fast, bistable and a slow, monostable mode.

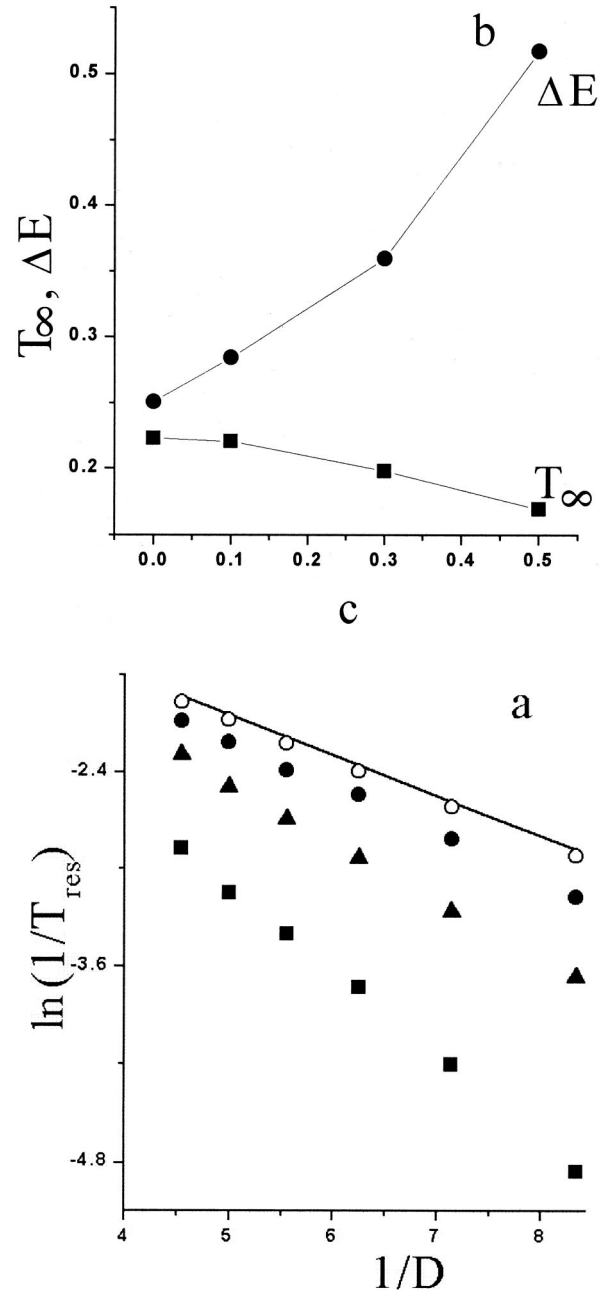


FIG. 7. Arrhenius plot of the dependence of mean residence time  $\langle T_{\text{res}} \rangle$  on noise intensity  $D$  for different values of coupling constant  $c$  at  $\tau = 0.001$ . (a) Solid line: Kramers' theory prediction [26]. Simulation results: open circles:  $c = 0$ ; full circles:  $c = 0.1$ ; triangles:  $c = 0.3$ ; squares:  $c = 0.5$ . (b) Dependence of apparent activation energy  $\Delta E$  and preexponential factor  $T_{\infty}$  (multiplied by a scaling factor of 10) on the coupling constant.

White, additive noise acts on the fast mode only; this could be generalized to the case where both subsystems are influenced by noise with different temperatures [12,27]. The coupling of the subsystems is symmetrically bidirectional, cooperative ( $c_1 = c_2 = c > 0$ ), and linear. The type of coupling—cooperative or antagonistic, bidirectional or unidirectional, linear or nonlinear—crucially determines the system dynamics. The present case is relevant e.g., to enzymatic reactions where allosteric effects are usually cooperative. Slow-mode decay is described here by a first-order process that is typical for biochemical reactions.

In the present study, noise is the key control parameter. Its value  $D$  serves in the first place to localize the slow-mode distribution  $P(Q;D)$  in phase space. While the fast mode is on average slaved to the slow mode [28], note however, that adiabatic elimination of  $q$  would also eliminate the slow-mode localization, noise-induced bistability and locking of transitions. Hence  $q$  is an essential mode and the model (2,3) is irreducible. The slow mode  $\langle Q \rangle$  exerts a key influence on the effective fast-mode potential  $V(q, \langle Q \rangle)$ , the effective fast-mode distribution  $P(q, \langle Q \rangle)$  and on the reactive kinetics of the fast mode.

The noise intensity serves to localize the slow-mode probability distribution  $P(Q;D)$  in phase space in a self-organized manner. With increasing  $D$ , the distribution changes from unimodal to bimodal (noise-induced bistability) and back to unimodal. In the case of unidirectional coupling (the fast mode affects only the slow mode, but not vice versa), the slow-mode probability density  $P(Q)$  is Gaussian and is always localized at the origin, while the fast-mode probability density  $P(q)$  is always bimodal and fully symmetric.

The coupling affects substantially also the fast mode. Below a critical noise level  $D < D_{cr}$ , the probability density  $P(q;D)$  is asymmetric, with the highest asymmetry at  $D = 0$ . This reflects the facts that  $\langle Q \rangle$  tends to  $V_{min}$  as  $D \rightarrow 0$ , and that the effective fast-mode potential  $V(q, \langle Q \rangle)$  is highly asymmetric in this region. If the initial conditions are chosen in a way that they correspond to the left (right) 2D attractor, the diffusion process will remain in the left (right) well for  $D < D_1$ . If one starts at the left (right) 2D attractor in the bistable case of  $D_1 < D < D_2$ , the system spends more time near the left attractor for  $c > 0$  (near the right attractor for  $c < 0$ ) and the probability density maximum is localized at the corresponding 2D wells.

Noise-induced bistability is generally associated with multiplicative noise [9–11]. Although in the present case the noise acts additively on the fast subsystem, the bidirectional coupling gives it an effectively multiplicative character.

The results indicate that the existence of well-separated time scales ( $\tau \approx 0.001$ ) combined with a temperature gradient and bidirectional, excitatory coupling gives rise to stochastic localization of macrostates. We believe that these results are generic and that they may be found in physical and biological systems possessing a hierarchy of time scales.

#### ACKNOWLEDGEMENT

This work was supported by the Natural Sciences and Engineering Research Council of Canada (NSERC).

#### APPENDIX A: APPROXIMATE STEADY STATE SOLUTION OF THE FOKKER-PLANCK EQUATION

The steady-state solution  $P^s(q, Q)$  of the Fokker-Planck equation corresponding to system (1) is given by

$$\begin{aligned} & \partial/\partial q[(q-q^3)+cQ]P^s(q, Q) \\ & - \tau(\partial/\partial Q)(-Q+cq)P^s(q, Q) + (D\partial^2/\partial q^2)P^s(q, Q) = 0, \end{aligned} \quad (\text{A1})$$

We approximate the PDF  $P^s(q, Q)$ , using the following factorization:

$$P^s(q, Q) = E(q, Q)P^s(Q), \quad (\text{A2})$$

where  $P^s(Q)$  is the unknown stationary PDF for the slow variable and the function  $E(q, Q)$  is chosen in such a way that it explicitly describes the contribution of the fast diffusion process and contains also a coupling term

$$E(q, Q) = \exp(-V(q)/D + cqQ/D), \quad (\text{A3})$$

where  $V(q) = -q^2/2 + q^4/4$ . This approximation is justified by the fact that the numerically obtained fast-mode distribution is close to the common 1D bimodal distribution for a bistable potential but is asymmetrical in its shape (Fig. 3). We found that this asymmetry is proportional to the coupling term  $cqQ$ .

Substituting (A2) and (A3) into (A1) and integrating first with respect to  $q$  and then to  $Q$ , the resulting expression for the desired quantity  $P^s(Q)$  is obtained as

$$P^s(Q) \sim \exp\left(-\int^Q \lambda(x)/\mu(x) dx\right), \quad (\text{A4})$$

where

$$\lambda(x) = \int_{-\infty}^{+\infty} E(q, x)\lambda_q(x, q) dq, \quad (\text{A5})$$

$$\mu(x) = \int_{-\infty}^{+\infty} E(q, x)\mu_q(x, q) dq, \quad (\text{A6})$$

and the functions  $\lambda_q(x, q)$  in (A5) and  $\mu_q(x, q)$  in (A6) are given by

$$\begin{aligned} \lambda_q(x, q) = & q(q^2-1)R(x, q) - cxR(x, q) + DR^2(x, q) + \tau(1 \\ & + cxq/D - cq^2), \end{aligned} \quad (\text{A7})$$

$$\mu_q(x, q) = \tau(x - cq), \quad (\text{A8})$$

where

$$R(x, q) = (cx + q - q^3)/D. \quad (\text{A9})$$

#### APPENDIX B: POSSIBLE SCALING TRANSFORMATION OF CONSIDERED SLOW-FAST SYSTEM TO A GRADIENT ONE

Introducing the new variables  $q' = \tau^{-1}q$ ,  $Q' = \tau Q$ ,  $t' = t$ , we can define the potential function by

$$V(q', Q'; c, \tau) = -q'^2/2 + \tau q'^4/4 + \tau/2 Q'^2 - c\sqrt{\tau} q' Q'. \quad (\text{B1})$$

This potential is shown in Fig. 2. It has a saddle point at the origin and two minima that are steep along the  $q'$  axis and very gradual along the  $Q'$  axis (since  $\tau \ll 1$ ). They are located at  $q'_{min} = \pm((1+c^2)/\tau)^{1/2}$ ,  $Q'_{min} = q'_{min} c \tau^{-1/2}$ . For  $Q' = 0$  the potential is the symmetric double-well potential

along the  $q'$  axis, but the slow-mode biases the fast mode and the corresponding potential  $V(q', Q' = \text{const})$  becomes increasingly asymmetric for  $Q' \neq 0$  with reactant well ( $q' > 0$ ) increasingly deeper than the product well, and *vice versa*.

The corresponding dynamic system

$$\partial q' / \partial t = -\partial V / \partial q' + \sqrt{(2D/\tau)} \xi(t), \quad (\text{B2a})$$

$$\partial Q' / \partial t = -\partial V / \partial Q', \quad (\text{B2b})$$

is a stochastic gradient system

- 
- [1] K. M. Christoffel and J. M. Bowman, *J. Chem. Phys.* **74**, 5067 (1981).
- [2] T. Fonseca, J. A. N. F. Gomes, P. Grigolini, and F. Marchesoni, *J. Chem. Phys.* **79**, 3220 (1983).
- [3] R. Lefever and J. Turner, *Phys. Rev. Lett.* **56**, 1631 (1986).
- [4] H. Treutein and K. Shulten, *Eur. Biophys. J.* **13**, 355 (1986).
- [5] S. J. Fraser and R. Kapral, *Phys. Rev. E* **56**, 2582 (1997).
- [6] P. Demchenko and V. A. Chinarov, *J. Mol. Liq.* **44**, 189 (1990).
- [7] V. A. Chinarov, Yu. B. Gaididei, V. N. Kharkyanen, and S. P. Sit'ko, *Phys. Rev. A* **46**, 5232 (1992).
- [8] C. R. Doering, *Phys. Rev. A* **34**, 2564 (1986).
- [9] W. Horsthemke and R. Lefever, *Noise Induced Transitions* (Springer, New York, 1984).
- [10] R. Graham and A. Schenzle, *Phys. Rev. A* **26**, 1676 (1982).
- [11] J. Boissonade, *Phys. Lett. A* **121**, 121 (1987).
- [12] P. Allegrini, P. Grigolini, and A. Rocco, *Phys. Lett. A* **233**, 309 (1997).
- [13] R. Landauer, *J. Appl. Phys.* **33**, 7 (1962).
- [14] M. Suzuki, *Physica A* **86**, 622 (1977).
- [15] B. Caroli, C. Caroli, and B. Roulet, *J. Stat. Phys.* **21**, 415 (1979).
- [16] R. Landauer and J. A. Swanson, *Phys. Rev.* **121**, 1668 (1961).
- [17] Z. Schuss and B. J. Matkovsky, *SIAM (Soc. Ind. Appl. Math.) J. Appl. Math.* **35**, 604 (1979).
- [18] D. G. Luchinsky, R. S. Mayer, R. Manella, P. V. E. McClintock, and D. L. Stein, *Phys. Rev. E* **82**, 1806 (1999).
- [19] R. Fitzhugh, *Biophys. J.* **1**, 445 (1961).
- [20] J. Nagumo, S. Arimoto, and S. Yoshizawa, *Proc. IRE* **50**, 2061 (1962).
- [21] N. V. Agudov, *Phys. Rev. E* **57**, 2618 (1998).
- [22] R. Wackerbauer, *Phys. Rev. E* **59**, 2872 (1999).
- [23] S. Faetti, L. Fronzoni, and P. Grigolini, *Phys. Rev. A* **32**, 1150 (1984).
- [24] J. P. Baltanas and K. M. Casado, *Physica D* **122**, 231 (1998).
- [25] R. L. Honeycutt, *Phys. Rev. A* **45**, 600 (1992).
- [26] P. Hanggi, F. Marchesoni, and P. Grigolini, *Z. Phys. B: Condens. Matter* **56**, 333 (1984).
- [27] M. Compiani, T. Fonseca, and P. Grigolini, *Chem. Phys. Lett.* **114**, 503 (1985).
- [28] H. Haken, *Synergetics, An Introduction*, 3rd ed. (Springer, Berlin, 1983).